

AMAL S.I. AHMED<sup>1</sup>, WAFAA A. GHANEM<sup>2</sup>, WALAA A. HUSSEIN<sup>1</sup>, GHALIA A. GABER<sup>1\*</sup>

## EVALUATION OF SOME INORGANIC ANIONS AND ORGANIC COMPOUNDS AS CORROSION INHIBITORS OF Cu-Zn ALLOYS IN H<sub>2</sub>SO<sub>4</sub> AND HNO<sub>3</sub> SOLUTIONS

Evaluation of inorganic and organic compounds as corrosion inhibitors of Cu-Zn alloys in H<sub>2</sub>SO<sub>4</sub> and HNO<sub>3</sub> solutions was studied using potentiodynamic and impedance spectroscopy along with scanning electron microscope (SEM) and energy dispersive X-Ray analyzer (EDX) investigations. The corrosion inhibition of Cu-Zn alloys was investigated in oxy acid solutions using inorganic potassium permanganate and di-hydrogen phosphate, amino acids as environmentally safe materials, commercial cooling water, and green tea extracts. Both potassium permanganate and di-hydrogen phosphate improve the corrosion resistance of Cu-Zn alloys. Phosphate appears more effective as corrosion inhibitor for Cu-Zn alloys than permanganate. The inhibition efficiency (IE%) of the different amino acids such as valine, leucine and lysine was also calculated. The experimental results have shown that amino acid-like lysine can be used as an efficient corrosion inhibitor for the Cu-Zn alloys in oxy acid solutions. This may be due to the presence of two amino groups adsorbed together. For lysine, inhibition efficiency, IE%, of ~87 and ~59 is for H<sub>2</sub>SO<sub>4</sub> and ~96.3 and 54.9 for HNO<sub>3</sub> for alloy I and II respectively are observed. Due to the composition of green water have a great effect on the inhibition action on Cu-Zn alloys which reaching 91.8 and 96.5% for Alloy I and 95.4 and 87.1% for Alloy II in 0.5 M H<sub>2</sub>SO<sub>4</sub> and HNO<sub>3</sub> respectively. Although benzotriazole, in cooling water, is an excellent inhibitor suitable for use in a wide variety of environments, it has toxic properties. So, much of the recent researches have focused on formulating new and more environmentally acceptable preservation solutions. The green tea, as plant extract, will be very environmentally friendly. The EDX confirm the formation of a protective layer on the Cu-Zn alloys containing aluminum in Alloy II. This sequence reflects the beneficial effects of Al in Alloy II. The presence of 2.43% Al in Alloy II improves the corrosion resistance due to the formation of thin, transparent, stable and self-healing Al<sub>2</sub>O<sub>3</sub> layer. This confirmed the results obtained from the potentiodynamic polarization measurements and EIS methods.

*Keywords:* Cu-Zn alloys; Oxy-acid Solution; Inhibition efficiency; Inorganic anions; Organic compounds

### 1. Introduction

Corrosion of copper and its alloys particularly in acidic media is an important industrial problem. Its alloys are widely used in industry because of their excellent electrical and thermal conductivity and are often used in heating and cooling system. Cu-Zn alloys have been widely used as tubing material for condensers and heat exchangers in various cooling water systems to condensate steam in turbine gas. Acid which is widely used for pickling, cleaning, descaling and etching of copper, on the other hand also contributes to the corrosion of metal surface. One of the best methods to reduce the rate of metallic corrosion is by the addition of inhibitors; even small concentrations can result in the decrease of the corrosion of the metal surface. Several conditions must be fulfilled for the selection of suitable

inhibitors: a) The cost and amount of the inhibitors. b) Long term toxicological effects on the environment and living species. c) The inhibitors availability and stability in the environment [1,2]. There are two types of corrosion inhibitors, inorganic and organic inhibitor. Protective action of inorganic inhibitor is related to the formation of oxide film or hardly soluble salt of the metal surface. On the other hand, protective action of organic inhibitors comes from the adsorption of the oxide film. The adsorbed inhibitor blocks either the anodic or cathodic reaction or both. The effect of the inhibitor may be due to charges in the electric double layer, by reducing the metal reactivity or by the inhibitor participation in partial electrode reaction and by formation of physical barrier. The adsorbed inhibitor may not cover the entire metal surface, but occupies sites which are electrochemically active and thereby reduced the extent of

<sup>1</sup> AL-AZHAR UNIVERSITY, FACULTY OF SCIENCE (GIRLS), CHEMISTRY DEPARTMENT, P.O. BOX: 11754, YOUSEF ABBAS STR., NASR CITY, CAIRO, EGYPT

<sup>2</sup> CENTRAL METALLURGICAL RESEARCH AND DEVELOPMENT INSTITUTE (CMRDI), P.O. BOX: 87, HELWAN, CAIRO, EGYPT

\* Corresponding author: ghaliiasaid@azhar.edu.eg



anodic or cathodic reactions or both. The corrosion rate will be decreased in proportion to the extent to which the electrochemically active sites are blocked by the adsorbed inhibitor [3]. A variety of organic compounds were studied for investigating their corrosion inhibition potential. Literature reveals that the presence of N, S and O in these organic compounds reported excellent inhibition efficiency. But, unfortunately they have the undesired toxic effect on environment, aquatic and animal life and expensive as well. Therefore, plants and natural product extracts have been posed to achieve the target of employing as a cheap, environmentally acceptable, abundant source, readily available and effective molecules having very high inhibition efficiency and low or zero environmental impact. It has been found that different organic compounds could be used as effective corrosion inhibitors during acid pickling process [4]. Currently the use of toxic material as corrosion inhibitors has been limited by agencies such as the U.S. Environmental Protection Agency (EPA), U.S. Department of Transportation (DOT) and Occupational Safety and Health Administration (OSHA). Although several synthetic compounds have been proved as excellent corrosion inhibitors, but most of them are highly toxic in nature and having a serious threats to both human and environment and often expensive and non-biodegradable in nature as well [5]. Based on environmental and safety issues of using corrosion inhibitors in industries has always been a global concern. The consequences of these toxic inhibitors may cause temporary or permanent damage like kidney or liver or disturbing biochemical or enzyme system in body. The toxicity may arise during synthesis or its applications. Therefore, the uses of non-toxic and natural products as corrosion inhibitors have become important because of the advantages of their environmentally friendly and biodegradable in nature, readily availability, renewable sources, and ecological aspects and can be synthesized by simple procedure with low cost [2-7]. It must be mentioned that the selection of inhibitors are based on the choice of the solid substrate and the environment to which it should be exposed. Regarding as the alternative of toxic-synthetic corrosion inhibitors with environmentally friendly types (eco-friendly, nature friendly or green), having a minimal or no harm on the environment, several researchers have proposed the use of eco-friendly materials in corrosive media. In order to investigate the inhibition efficiency of these eco-friendly inhibitors in various acid medium, there are several experimental methodologies have been employed.

This article focuses on the application of various inorganic anion, organic compounds, commercial cooling water and efficiency of natural products which are used as co-friendly corrosion inhibitors for the corrosion protection of copper alloys in hydrochloric acid pickling processes. We evaluate the role of inorganic anion ( $\text{MnO}_4^-$  and  $\text{PO}_4^{3-}$ ) and organic compounds (amino acid, green water, green tea) in the retardation of corrosion of Cu-Zn alloys (I and II) in 0.5 M  $\text{H}_2\text{SO}_4$  and  $\text{HNO}_3$  acid solutions using potentiodynamic polarization measurements and electrochemical impedance spectroscopy.

## 2. Experimental procedure

### 2.1. Materials

Cylindrical specimen was taken from a rod of two types of the commercial copper alloys with the chemical composition (wt%): 83.47 Cu; 14.66 Zn; 0.67 Si; 0.50 Ca for alloy I (Cu-Zn) and 62.98 Cu; 31.86 Zn; 0.94 Si; 1.08 Mn; 0.50 Al for alloy II (Cu-Zn-Al). These alloys were prepared by Central Metallurgical Research and Development Institute. The rod was mounted in a glass tube of appropriate diameter using epoxy resin leaving a specified circular surface area ( $1\text{cm}^2$ ) to contact the electrolyte.

### 2.2. Surface pretreatment of the electrodes

Before each experiment, the surface of the electrode was mechanically polished with successive grades of 120 up to 1200 emery papers till the surface appears as a bright mirror. The electrodes were then rinsed several times with deionized water and degreased with acetone and immersed directly in the test solution.

### 2.3. Electrolytic cell

The cell glass used in potentiodynamic and impedance measurements has five opening in the main joint of the vessel, three of them for the following three electrodes, the working electrode, the Pt counter electrode and the Ag/AgCl reference electrode and the other two as inlet and outlet of the gas. The cell was of double walled with two opening for the circulation of the thermostated water.

### 2.4. Electrolytes

The chemicals used to prepare all solutions were Analar grade reagents. All solutions were freshly prepared by deionized water. The electrolytes used were different concentrations of  $\text{H}_2\text{SO}_4$  and  $\text{HNO}_3$ , (0.01 M – 1 M) as shown in the paper title; studies of corrosion and electrochemical behavior of Cu-Zn Alloys in  $\text{H}_2\text{SO}_4$  and  $\text{HNO}_3$  acid solutions by details [1].

### 2.5. Inhibitors

Inhibitor solutions used were:

- Inorganic inhibitors: Different concentrations of some inorganic salts like  $\text{NaH}_2\text{PO}_4$  and  $\text{KMnO}_4$  (0.01 M – 0.1 M). These additives were chemically pure grades and obtained from Aldrich.
- Organic inhibitors: Different concentration of amino acids (valine, leucine and lysine) used as environmentally safe materials. Their molecular structure is shown in Figure 1.

- c. Commercial inhibitor: Different concentrations of commercial cooling water inhibitor (green water which contains ethylene glycol, sodium tetraborate and dye beside benzotriazole).
- d. Natural products: Different concentrations of Green tea extracts (*Camellia Sinensis*) were tested as corrosion inhibitor for Cu-Zn alloys. The green tea extract was obtained directly from the tea bags of Lipton green tea. Stock solutions of the inhibitor extract were prepared by boiling 1.5 grams of dried tea bags in 250 ml of double distilled water for 30 min. The extract was left all night, then filtered and completed to 1000 ml with double distilled water. The green tea extracts were analyzed by IR spectroscopy for the identification of the functional groups. Figure 2 shows the IR absorption spectrum of the green tea extracts and the typical functional groups of catechin namely O-H, C=C (for aromatic rings), and C-O that were evidenced at 3500 to 3200, 1600, and 1150 to 1010  $\text{cm}^{-1}$ , respectively [8].

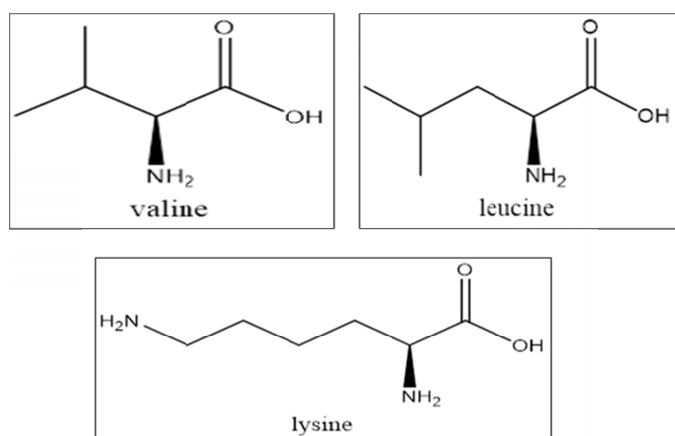


Fig. 1. Molecular structure of amino acids tested

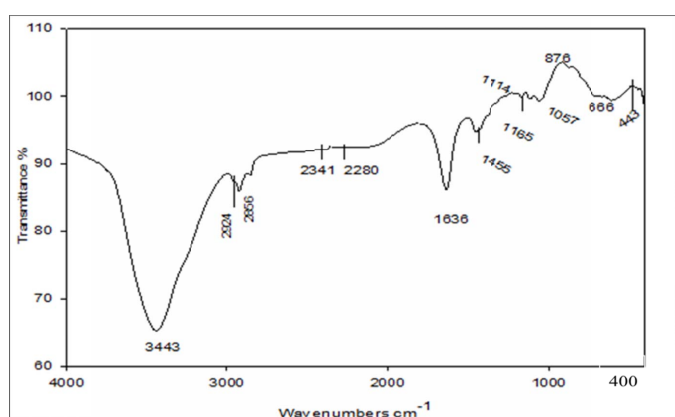


Fig. 2. IR spectra of green tea extracts

## 2.6. Electrochemical measurements

Two different electrochemical methods were used to evaluate the corrosion behavior of Cu-Zn alloys in 0.5 M  $\text{H}_2\text{SO}_4$  or  $\text{HNO}_3$  acid solution in the absence and presence of different inhibitors. The potentiodynamic polarization measurements

and electrochemical impedance spectroscopy were performed using the Voltalab 40 Potentiostat PGZ301 made in Germany. The Volta Master 4 software is designed to measure and analyze corrosion rate. The measurements, processing, storage, retrieval and analysis of data generated has been automated.

### 2.6.1. Potentiodynamic polarization

The potentiodynamic polarization measurements of Cu-Zn alloys (I, II) in the absence and presence of examined compounds were started at  $-800 \text{ mV}_{\text{Ag}/\text{AgCl}}$  up to  $1000 \text{ mV}_{\text{Ag}/\text{AgCl}}$  with scanning rate  $2 \text{ mV}/\text{sec}$ . The corrosion rate, C.R. ( $\mu\text{m}$  consumption of copper alloys per year) can be computed using Faraday's Law as follows [9]:

$$C.R. (Mm/year) = 3.3 I_{corr} \frac{M}{zd} \quad (1)$$

Where;  $z$  = ionic charge (2 for Cu),  $M$  = atomic weight of copper (63.546),  $d$  = density of copper,  $8.96 \text{ g}/\text{cm}^3$ , and  $I_{corr}$  = corrosion current density,  $\mu\text{A}/\text{cm}^2$ . From the corrosion rate values, the inhibition efficiency (IE%) was calculated employing Eq. (2) [8]:

$$IE \% = \theta \times 100 \equiv \frac{[CR - CR_{inh}]}{CR} \times 100 \quad (2)$$

where  $CR$  and  $CR_{inh}$  are the corrosion rates in the absence and presence of inhibitor respectively.

### 2.6.2. Electrochemical Impedance spectroscopy (EIS)

Electrochemical impedance spectroscopy measurements of the two Cu-Zn alloys were carried out in frequency range from (100 kHz to 100 mHz) with amplitude of 10 mV peak-to-peak using ac signals at open circuit potential. The inhibition efficiencies (IE%) and the surface coverage ( $\theta$ ) obtained from the impedance measurements are defined by the following equation (3) [8].

$$IE \% = \theta \times 100 \equiv \frac{[R_{ct}(inh) - R_{ct}]}{R_{ct}(inh)} \times 100 \quad (3)$$

Where  $R_{ct}$  and  $R_{ct}(inh)$  are the charge transfer resistance in the absence and presence of inhibitor, respectively. The main parameters deduced from the analysis of Nyquist diagram are the resistance of charge transfer  $R_{ct}$  (diameter of high frequency loop) and the capacitance of double layer  $C_{dl}$  which is defined as [10]:

$$C_{dl} = (2\pi R_{ct} F_{max})^{-1} \quad (4)$$

where  $F_{max}$  is the maximum frequency at which the imaginary component ( $Z_{imag}$ ) of the impedance is a maximum. Since the electrochemical theory assumed that  $1/R_{ct}$  is directly proportional to the capacity of double layer [11]. According to circuit theory [1], an impedance plot obtained for a given electrochemical system can be correlated to one or more equivalent circuit. Figure 3 show equivalent circuit model for the studied system.

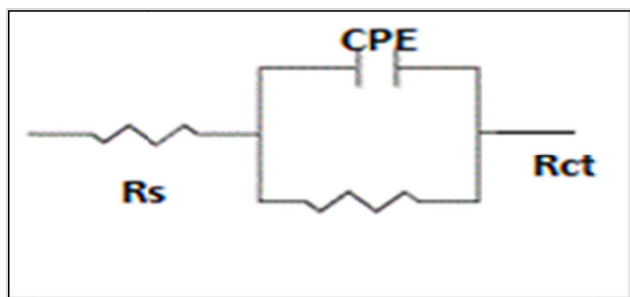


Fig. 3. Suggested equivalent circuit model for the studied system

## 2.7. Spectroscopic analysis

The SEM images were obtained by using SEM Model Quanta 250 FEG (Field Emission Gun) attached with EDX Unit (Energy Dispersive X-ray Analyses), with accelerating voltage 30. SEM and EDX analyses were used to define the morphology of surface attack and the chemical composition of corrosion products on Cu-Zn alloys from testes terminated just after the film breakdown occurred.

## 3. Results and discussion

### 3.1. Potentiodynamic polarization measurements

Figure 4 studied the anodic and cathodic curves of the Cu-Zn alloys in aerated 0.5 M of  $\text{H}_2\text{SO}_4$  and  $\text{HNO}_3$  in the absence and presence of 0.1 M  $\text{KMnO}_4$  or  $\text{NaH}_2\text{PO}_4$ , at 25°C. The values of corrosion potential  $E_{corr}$ , corrosion current density  $I_{corr}$ , cathodic and anodic Tafel slope ( $\beta_a$  and  $\beta_c$ ), corrosion rate and inhibition efficiency  $\text{IE}\%$  are listed in Table 1-4. The result of Figure 4 and Tables 1-4 indicate that upon adding  $\text{MnO}_4^-$  and  $\text{PO}_4^{3-}$  ions to  $\text{H}_2\text{SO}_4$  or  $\text{HNO}_3$  solutions, the corrosion current density ( $I_{corr}$ ) and the corrosion rate decreased. The slopes of the anodic and cathodic Tafel lines ( $\beta_a$  and  $\beta_c$ ) changed which indicate that the used inhibitors have an effect on the mechanism of the dissolution of the two Cu-Zn alloys. The behavior of the Cu-Zn alloys (I and II) in aerated  $\text{MnO}_4^-$  or  $\text{PO}_4^{3-}$  ions solutions exhibited an active passive behavior. This can clear from cathodic current – potential curves give rise to parallel Tafel lines indicating that the cathodic current density decreases with the inhibitors more over a small effect is observed on the anodic portions. This result indicates that investigated inhibi-

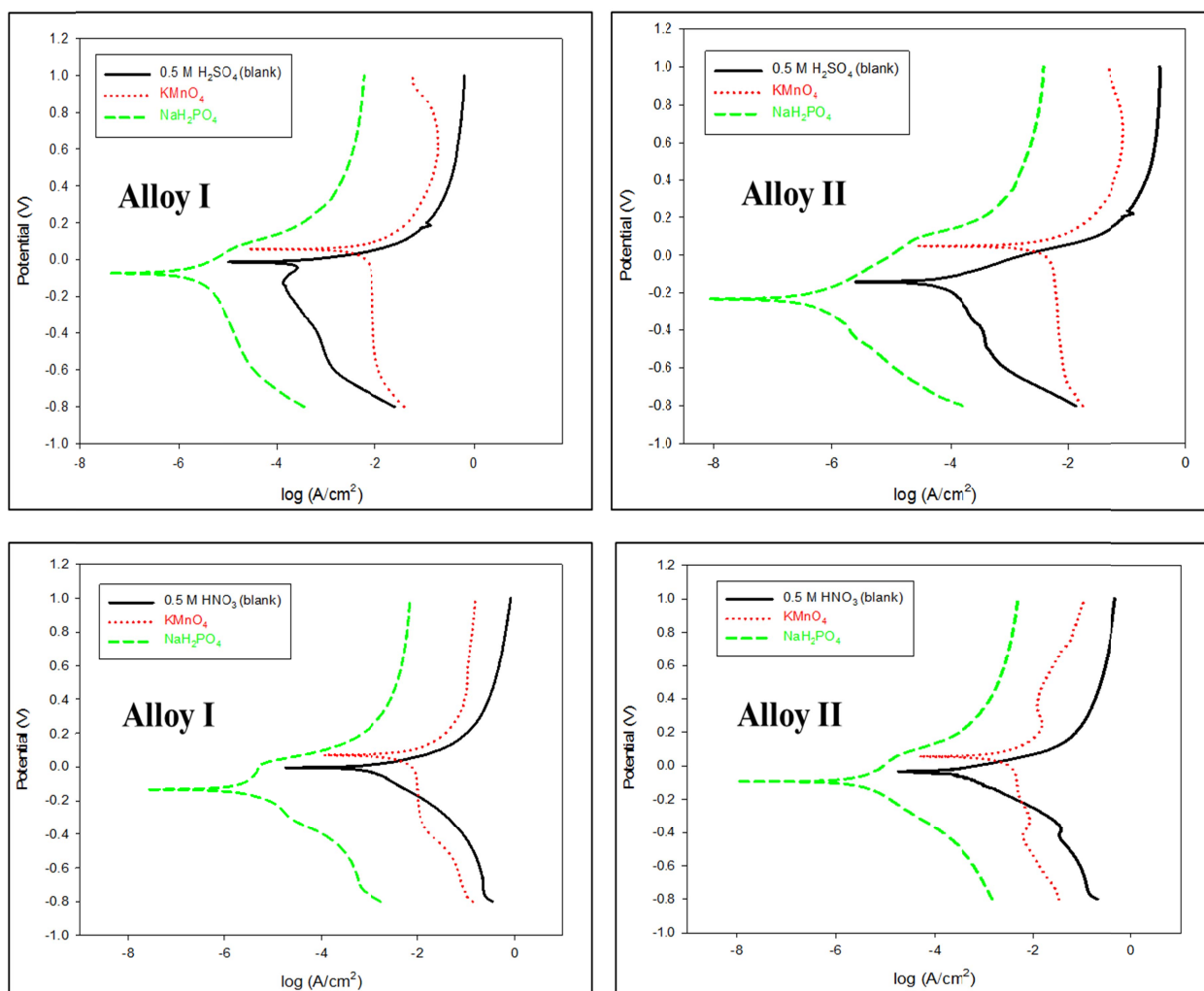


Fig. 4. Anodic and cathodic potentiodynamic polarization curves of two Cu-Zn alloys in aerated 0.5 M of  $\text{H}_2\text{SO}_4$  and  $\text{HNO}_3$  in the absence and presence of 0.1 M inorganic anion, at 25°C



TABLE 1

Corrosion parameters for Alloy I in 0.5 M H<sub>2</sub>SO<sub>4</sub> solution in the absence and presence of all investigated inhibitors

Inhibitor		$E_{corr}$ mV	$I_{corr}$ mA/cm <sup>2</sup>	$\beta_a$ mV	$\beta_c$ mV	C.R. mm/y	IE %
0.5 M H <sub>2</sub> SO <sub>4</sub> (Blank)		-52.9	0.1687	38.1	-302.8	1.960	—
0.1 M inorganic anion	KMnO <sub>4</sub>	57.9	0.02269	58.0	-122.4	0.263	86.5
	NaH <sub>2</sub> PO <sub>4</sub>	-76.3	0.01549	144.3	-201.8	0.180	90.8
10 <sup>-2</sup> M amino acid	Valine	-81.5	0.0238	43.6	-52.1	0.2771	85.8
	Leucine	-75.9	0.03175	72.6	-91.1	0.3689	81.1
	Lysine	-93.3	0.02169	16.7	-28.6	0.2520	87.1
50% Green inhibitors	Green water	-70.6	0.01381	117.9	-131.7	0.1605	91.8
	Green tea	-47.3	0.0145	84.8	-112.5	0.1691	91.3

TABLE 2

Corrosion parameters for Alloy II in 0.5 M H<sub>2</sub>SO<sub>4</sub> solution in the absence and presence of all investigated inhibitors

Inhibitor		$E_{corr}$ mV	$I_{corr}$ mA/cm <sup>2</sup>	$\beta_a$ mV	$\beta_c$ mV	C.R. mm/y	IE %
0.5 M H <sub>2</sub> SO <sub>4</sub> (Blank)		-144.6	0.0282	50.0	-86.4	0.328	—
0.1 M inorganic anion	KMnO <sub>4</sub>	44.0	0.0112	59.9	-84.4	0.1307	60.1
	NaH <sub>2</sub> PO <sub>4</sub>	-235.2	0.00338	134.3	-185.8	0.0393	88.0
10 <sup>-2</sup> M amino acid	Valine	-126.8	0.01617	80.1	-96.2	0.1879	42.7
	Leucine	-145.4	0.0138	68.1	-100.4	0.1604	51.0
	Lysine	-148.7	0.01149	72.5	-112.9	0.1335	59.2
50% Green inhibitors	Green water	-79.3	0.00129	138.7	-144.7	0.01506	95.4
	Green tea	-311.9	0.0058	180.8	-151.5	0.0678	79.3

TABLE 3

Corrosion parameters for Alloy I in 0.5 M HNO<sub>3</sub> solution in the absence and presence of all investigated inhibitors

Inhibitor		$E_{corr}$ mV	$I_{corr}$ mA/cm <sup>2</sup>	$\beta_a$ mV	$\beta_c$ mV	C.R. mm/y	IE %
0.5 M HNO <sub>3</sub> (Blank)		-9.3	1.005	65.3	-173.1	11.68	—
0.1 M inorganic anion	KMnO <sub>4</sub>	63.9	0.6414	53.4	-93.4	7.45	36.2
	NaH <sub>2</sub> PO <sub>4</sub>	-137.9	0.5620	39.8	-39.8	6.530	44.0
10 <sup>-2</sup> M amino acid	Valine	-121.1	0.4118	56.8	-36.5	0.4785	95.0
	Leucine	-38.4	0.8357	54.5	-155.7	0.9712	91.6
	Lysine	-92.2	0.3656	21.0	-41.0	0.4248	96.3
50% Green inhibitors	Green water	-53.0	0.03427	33.1	-47.5	0.398	96.5
	Green tea	-140.7	0.0540	211.9	-169.5	0.628	94.6

TABLE 4

Corrosion parameters for Alloy II in 0.5 M HNO<sub>3</sub> solution in the absence and presence of all investigated inhibitors

Inhibitor		$E_{corr}$ mV	$I_{corr}$ mA/cm <sup>2</sup>	$\beta_a$ mV	$\beta_c$ mV	C.R. mm/y	IE %
0.5 M HNO <sub>3</sub> (Blank)		-45.9	0.3337	61.4	-129.3	3.877	—
0.1 M inorganic anion	KMnO <sub>4</sub>	51.2	0.2626	181.0	-458.4	3.052	21
	NaH <sub>2</sub> PO <sub>4</sub>	-98.0	0.07412	34.1	-45.8	0.8617	77.7
10 <sup>-2</sup> M amino acid	Valine	-52.6	0.1850	92.7	-113.8	2.149	44.5
	Leucine	-257.3	0.1716	160.7	-82.0	1.994	48.6
	Lysine	-28.9	0.1508	17.0	-28.6	1.75	54.9
50% Green inhibitors	Green water	-100.2	0.0428	153.0	-113.6	0.4978	87.1
	Green tea	-197.9	0.0538	319.3	-117.8	0.626	83.8

tor is adsorbed on the metal surface on the cathodic sites and hence inhibition occurs, we remark that the inhibitor acts on the anodic portion and the anodic current density is reduced. It seems also that the presence of the inhibitor change slightly the

corrosion potential values in no definite direction. Depending on the surface observation and literature review [12], it is generally accepted that in the absence of the corrosion inhibitor, the acidic solution is always in contact with the metal and porous

film surface causing corrosion as a result of metal dissolution, whereas in the presence of inhibited solution, the active or open sites in the porous film are almost blocked by the adsorption of the inhibitor resulting a barrier or a passive layer suppress the further corrosion.

$\text{KMnO}_4$  is widely used in passivation bath, in acid pickling and in chemical descaling. The reactions are governed by pH of the medium. Permanganate, when mixed with acid or alkali, is one of the strongest oxidizing agents known. It oxidizes the metal and reduced to manganese dioxide. The oxidation reaction of permanganate in acidic media can be represented by the following equation:



Further experiments indicated that the instantaneous reaction between  $\text{MnO}_4^-$  and Cu alloys varies with time exposure. Initially, the rate of the corrosion between  $\text{MnO}_4^-$  and Cu alloys was high, but as the reaction time precedes the oxide film which formed on the metal surface hinders further corrosion. The thickness and composition of the manganese oxide film formed over the metal surface thus varied with time [13]. Under the conditions prevailing in the permanganic acid medium and by visual investigation, it was observed that two distinct layers of oxide film were formed. The inner layer was bluish in color, thin and

adherent, whereas, the outer oxide was loose, brownish black in color and contained manganese oxide. During the processes, the  $\text{MnO}_4^-$  (Mn (VII)) converted to Mn (IV) or Mn (III). The Mn (IV) exists as manganese dioxide under the process conditions with solution pH being 2.7 and electrochemical potential around 0.9-1.0 V [13]. Hence, a uniform manganese dioxide deposit was seen on Cu-Zn alloys. The thickness of the film deposited over the Cu-Zn alloys surface increased with time leading to increase in inhibition efficiency, IE, reaching with  $\text{H}_2\text{SO}_4$  acid to ~86 and 60 and with  $\text{HNO}_3$  acid to ~36 and 21 for Alloy I and II, respectively.

For Cu-Zn alloys in acidic media, the presence of  $\text{PO}_4^{3-}$  has more profound effect on the rate of the anodic than on cathodic reaction. This effect clears from table which found  $\beta_a$  144.3 mV and 134.3 mV for Alloy I and II, respectively in  $\text{H}_2\text{SO}_4$  acid. Visual investigation of the Cu-Zn alloys in absence and presence of inorganic inhibitors also show the presence of  $\text{PO}_4^{3-}$  has more profound than permanganate. The anodic reaction is supported by the selective dissolution of zinc and subsequently the simultaneous dissolution of zinc and copper [14]. Figure 4 show that at a certain anodic current, the potential increases (in the positive direction). This attributed to the precipitation on the brass surface of thicker and hence more protective layers of phosphate complex in solution of  $\text{PO}_4^{3-}$ .

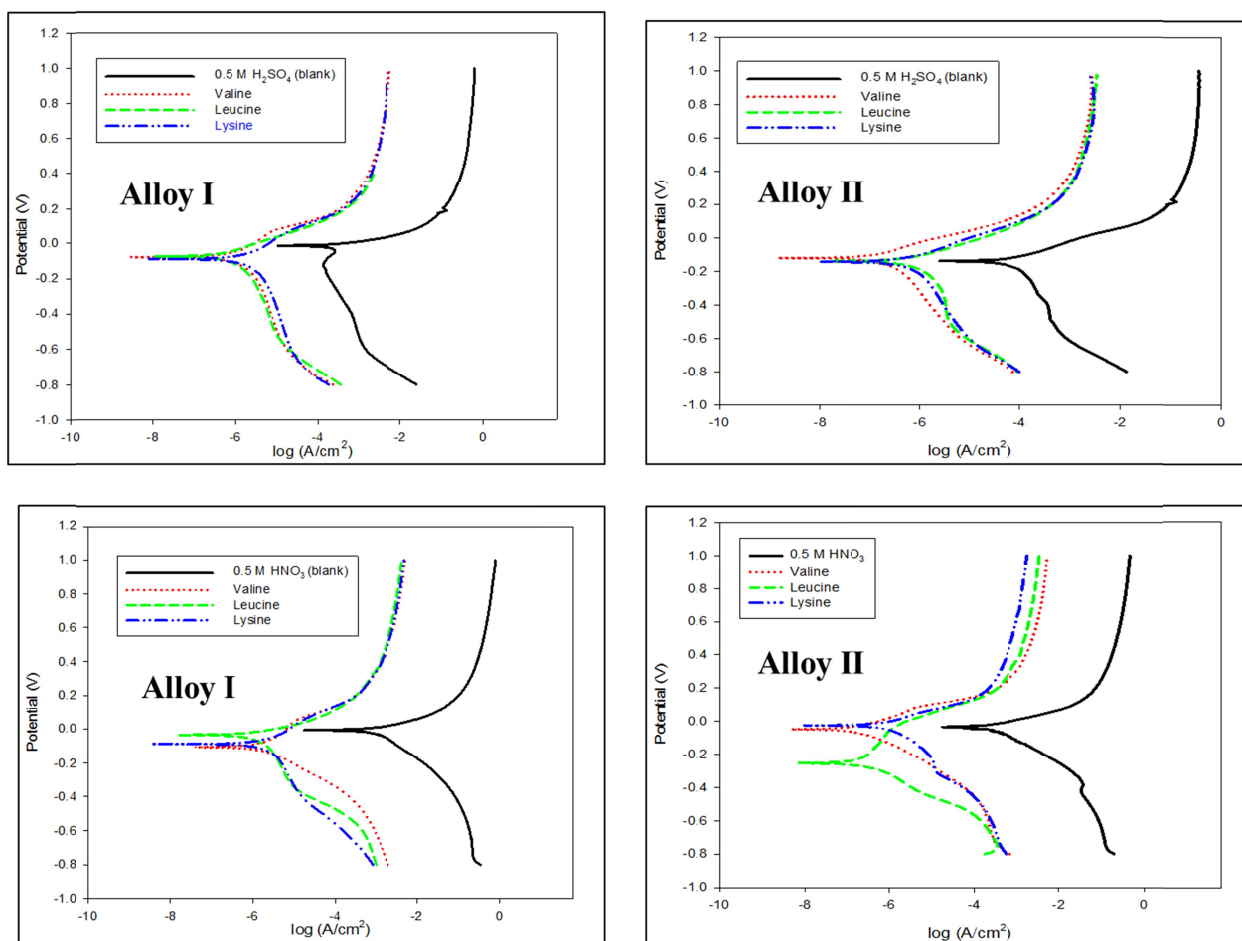
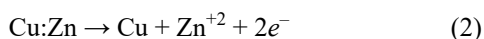


Fig. 5. Anodic and cathodic potentiodynamic polarization curves of two Cu-Zn alloys in 0.5 M of  $\text{H}_2\text{SO}_4$  and 0.5 M  $\text{HNO}_3$  solutions in the absence and presence of 0.01 M amino acid

Upon dezincification the Cu-Zn alloys undergoes the following reactions:



After the outer surface of the Cu-Zn alloys is depleted of Zn and enriched in Cu, the Cu-Zn alloys undergo simultaneous dissolution of both Zn and Cu [15]. In the presence of phosphate ions, the precipitation of  $\text{Zn}_3(\text{PO}_4)_2$  on the dissolving alloy surface becomes a distinct possibility. This is particularly true at short times where the anodic dissolution reaction produces only zinc ions [15]. The  $\text{Zn}_3(\text{PO}_4)_2$  is precipitated at the regions where the alloy, otherwise, undergoes further dezincification. Hence, the formation of protective layers of phosphate complexes is increased leading to the increased of inhibition efficiency, IE%, values reaching with  $\text{H}_2\text{SO}_4$  acid 91, 88% and with  $\text{HNO}_3$  acid 44, 78% for Alloys I and II, respectively.

The anodic and cathodic potentiodynamic polarization curves of the Cu-Zn alloys in 0.5 M of  $\text{H}_2\text{SO}_4$  and 0.5 M  $\text{HNO}_3$  solutions in the absence and presence of  $10^{-2}$  M of valine, leucine and lysine are shown in Figure 5. The potentiodynamic parameters together with percent of inhibition efficiency (IE%) of the Cu-Zn alloys are given in Tables 1-4. Inspection of these figures reveal that cathodic polarization curves gave rise to parallel Tafel lines, indicating that the hydrogen evolution reaction is activation controlled and the presence of various amino acids tested does not affect the mechanism of this process. It was clearly seen that, the presence of amino acids compound at  $10^{-2}$  reduce the corrosion rate of two Cu-Zn alloys in  $\text{H}_2\text{SO}_4$  or  $\text{HNO}_3$  solution. The corrosion rate reducing in the presence of tested amino acids due to (1) slowing the anodic and/or cathodic reaction (2) slowing the diffusion of aggressive species to the metal surface and (3) decreasing the electrical resistance of the metal surface [2]. All amino acids exhibit a catalytic effect on anodic domain [16]. In acidic media,  $\text{NH}_2$  of amino acids molecule is readily protonated to form  $\text{NH}_3^+$ , also the addition of valine and leucine leads to decrease in corrosion current density comparing to blank 0.5 M  $\text{H}_2\text{SO}_4$  or 0.5 M  $\text{HNO}_3$ . This phenomenon is essentially due to the presence of aliphatic radical R of valine and leucine. But when the radical contains heteroatom as N a decrease of corrosion current density in the presence of lysine at  $10^{-2}$  M was noted.

For lysine, adsorption occurs via the amino groups and inhibition efficiency, IE%, of ~87 and ~59 is for  $\text{H}_2\text{SO}_4$  and ~96.3 and 54.9 for  $\text{HNO}_3$  for alloy I and II respectively are observed. Among the amino acids studied lysine, showed the highest inhibition. This may be due to the presence of two amino groups adsorbed together [17]. The cathodic reaction, hydrogen evaluation, is influenced by the presence of amino acids. There appears to be no correlation between inhibition efficiency and the cathodic Tafel slope. This would indicate that the presence of the amino acids does not change the cathodic reaction mechanism, but that adsorption of the compounds acts to block

portions of the electrode. The examination of polarization curves shows that also the chain length of the amino acid molecules or the branched structures did not show remarkable effect as was recorded previously in acidic solution [18].

The anodic and cathodic potentiodynamic polarization curves of the two Cu-Zn alloys in 0.5 M of  $\text{H}_2\text{SO}_4$  and  $\text{HNO}_3$  solutions in the absence and presence of green water and green tea are shown in Figure 6. The corrosion parameters and percent of inhibition efficiency (IE%) of the Cu-Zn alloys are tabulated in Table 1-4. It is clear from Figure 6 and Tables 1-4 that the decrease in the corrosion current density which attributed to the inhibition efficiency of green water and green tea extent on the cathodic part of polarization curves through the reaction of hydrogen ions  $\text{H}^+$  and also its effectiveness on the anodic part due to adsorption of the green water or extract components of green tea on the surface of copper alloy which form a barrier hinders the process of hydrogen gas evolution and metal dissolution. Due to the composition of green water which contains ethylene glycol, sodium tetraborate and dye beside benzotriazole, this have a great effect on the inhibition action on the two Cu-Zn alloys which reaching 91.8 and 96.5% for Alloy I and 95.4 and 87.1% for Alloy II in 0.5 M  $\text{H}_2\text{SO}_4$  and  $\text{HNO}_3$  respectively.

Commercial cooling water contains benzotriazole, which is an efficient corrosion inhibitor for copper and its alloys in a wide variety of environments. Benzotriazole is an organic compound consisting of benzene and triazole rings with a formula of  $\text{C}_6\text{H}_5\text{N}_3$  which can exist in different tautomeric forms [19]. Benzotriazole can act as a weak acid by releasing a proton or a base by accepting a proton to one of the nitrogen lone pairs of electrons. On other hand, benzotriazole can utilize the lone pairs of electrons existing on nitrogen atoms to bond itself to copper surface. In this way, a coordination compound can be formed on the copper surface which acts as an inhibitor against corrosion. This makes benzotriazole one of the most efficient inhibitors for corrosion of copper and its alloys in different media [19]. Generally, benzotriazole acts as an anodic corrosion inhibitor via its physisorption on the copper surface. While changing in the anodic and cathodic Tafel slopes ( $\beta_a$  and  $\beta_c$ ) Tables 1-4 conforming that this inhibitor can control both anodic as well as cathodic reactions and act as mixed inhibitors as shown by other authors [20].

Although benzotriazole, in cooling water, is excellent inhibitor suitable for use in wide variety of environments, it has toxic properties. So, much of recent researches have focused on formulating new and more environmentally acceptable preservation solutions [20]. The green tea, as plant extract, will be very environmentally friendly. The green tea extracts were analyzed by IR spectroscopy Figure 2 showing that, the typical function groups of catechin namely O-H, C=C (for aromatic rings) and C-O. It is clear from Tables 1-4 that the inhibition efficiency, IE%, for the Cu-Zn alloys for 50% green tea extract is reached 91.3 and 94.6 for Alloy I while is reached 79.3 and 83.8 for Alloy II in 0.5 M  $\text{H}_2\text{SO}_4$  and  $\text{HNO}_3$  acids respectively. Tea component molecules contain many compounds such as, caffeine, alkaloids, phenolic substances, tannins, fats, flavonoids amino

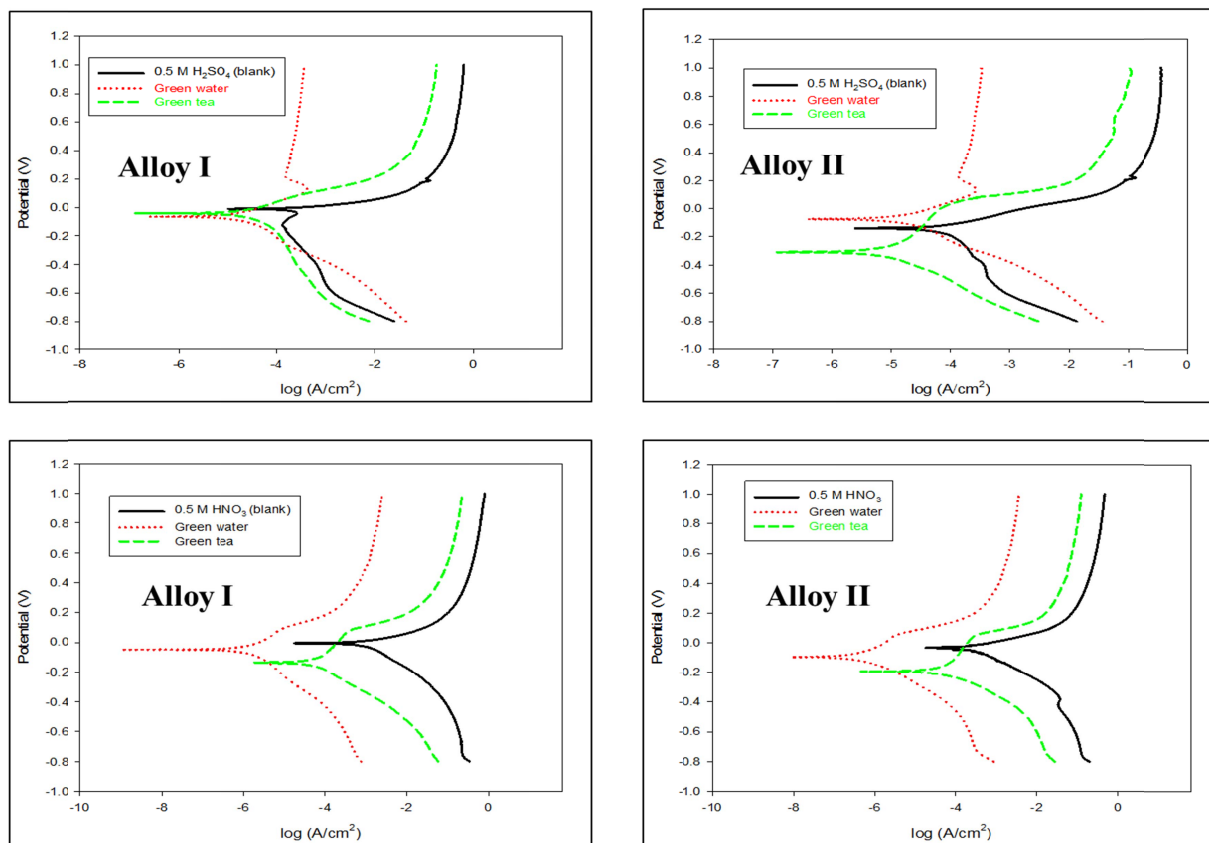


Fig. 6. Anodic and cathodic potentiodynamic polarization curves of two Cu-Zn alloys in 0.5 M of  $\text{H}_2\text{SO}_4$  and  $\text{HNO}_3$  solutions in the absence and presence of 50% green water and green tea

acids sterols and vitamin C [8], so green tea extract possesses several heteroatoms containing active constituents and therefore there may be a synergism between the molecules an accounting for the good inhibition efficiencies. The functional groups of the green tea extract are playing important role during the adsorption process. The process of adsorption is the process of replacing between extract molecules.

### 3.2. Electrochemical impedance spectroscopy

Electrochemical impedance is widely used for investigation of the corrosion inhibition processes. This method is an influential application in obtaining more information on the kinetics of the electrode processes and on the surface properties of the system investigated. This method delivers more reliable results because it does not disturb the double layer at the metal / solution interface [21]. The impedance data points of the Cu-Zn alloys in the presence of different inhibitor were analyzed using the equivalent circuit shown in Figure 3. This equivalent circuit which has been previously reported [11], fitted well with our experimental results. The calculated equivalent circuit consists of the ohmic resistance of the corrosion product films and the solution enclosed between the working electrode and the reference electrode,  $R_s$ , the charge transfer resistance represented by  $R_{ct}$ , where the values signify the electron transfer across the surface and is inversely proportional to corrosion rate [22].

Figure 7 show the impedance complex diagram of two Cu-Zn alloys in both aerated 0.5 M of  $\text{H}_2\text{SO}_4$  and  $\text{HNO}_3$  acid solutions in presence of each  $\text{MnO}_4^-$  and  $\text{PO}_4^{3-}$  at concentration 0.1 M. The electrochemical impedance parameters together with percent inhibition efficiency are tabulated in Table 5 and 6. The impedance diagram in these Figure 7 and Table 5 and 6 shows that the charge transfer resistance of two Cu-Zn alloys in both 0.5 M of  $\text{H}_2\text{SO}_4$  and  $\text{HNO}_3$  increase in the presence of  $\text{PO}_4^{3-}$  than  $\text{MnO}_4^-$ . Electrochemical theory shows that the reciprocal of the charge transfer resistance is proportional to the corrosion rate [22]. The corrosion rate of two Cu-Zn alloys in  $\text{H}_2\text{SO}_4$  and  $\text{HNO}_3$  is high in  $\text{MnO}_4^-$  than that in presence of  $\text{PO}_4^{3-}$ . This indicates that  $\text{PO}_4^{3-}$  is more efficient than  $\text{MnO}_4^-$ . This is in good agreement with potentiodynamic polarization measurements.

The corrosion behavior of two Cu-Zn alloys in 0.5 M  $\text{H}_2\text{SO}_4$  or  $\text{HNO}_3$  acid solution in the absence and presence of different amino acid (Valine, Leucine and Lysine) at  $10^{-2}$  M also investigated by the electrochemical impedance spectroscopy at  $25^\circ\text{C}$  as shown in Figure 8. The impedance parameters and percent of inhibition efficiency are presented in Table 5 and 6. The curves show a similar type of Nyquist plots for two Cu-Zn alloys in the presence of inhibitor. The existence of single semicircle showed the single charged transfer process during dissolution which is unaffected by the presence of inhibitors molecules. Deviations from perfect circular shape are often referred to the frequency dispersion of interfacial impedance, which arises due to surface roughness, impurities, dislocations, grain boundaries,

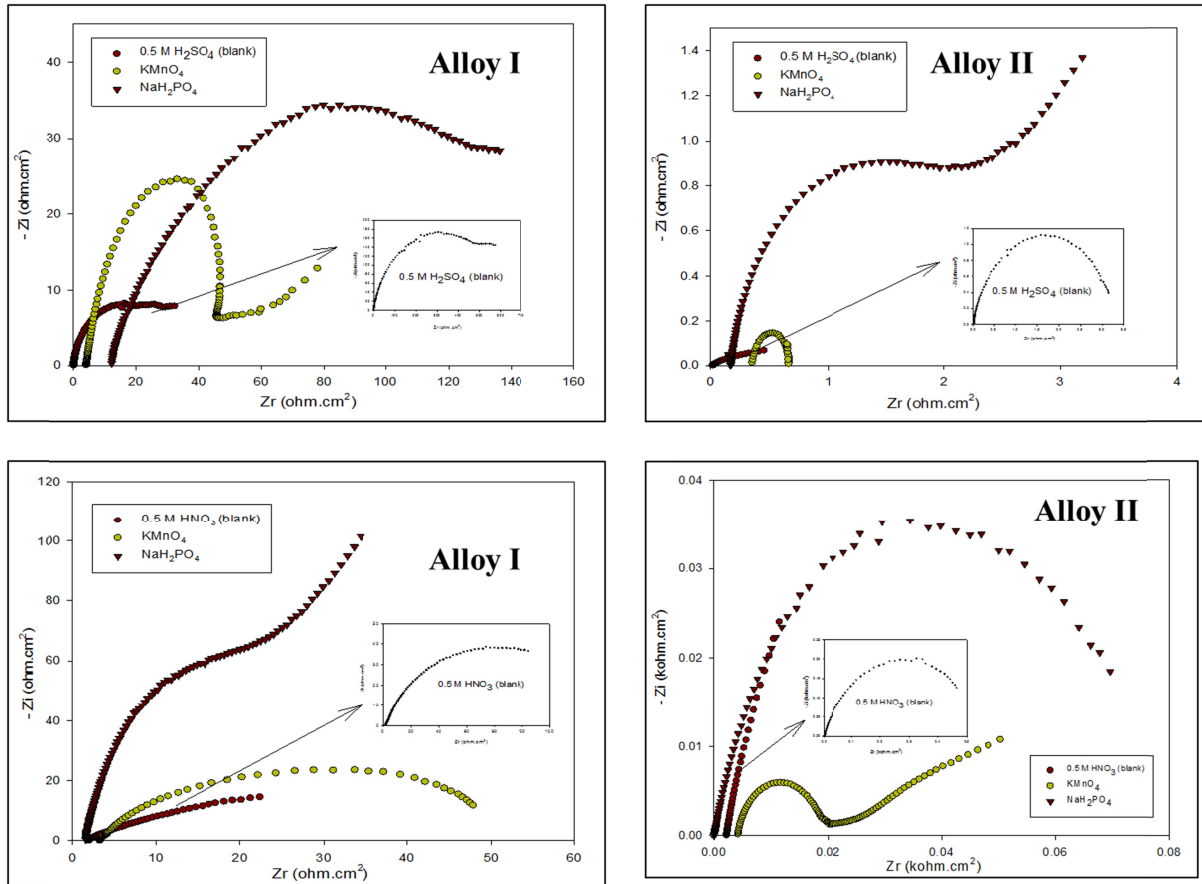


Fig. 7. Nyquist plot for Alloy I in 0.5 M HNO<sub>3</sub> solution in the absence and presence of 0.1 M inorganic anion

TABLE 5

Electrochemical impedance parameters for Cu-Zn alloys in 0.5 M H<sub>2</sub>SO<sub>4</sub> solution in the absence and presence of all investigated inhibitors

Inhibitors		Alloy (I)			Alloy (II)		
		$R_{ct}$ kohm.cm <sup>2</sup>	$C_{dl}$ μF/cm <sup>2</sup>	IE %	$R_{ct}$ kohm.cm <sup>2</sup>	$C_{dl}$ μF/cm <sup>2</sup>	IE %
0.5 M H <sub>2</sub> SO <sub>4</sub> (Blank)		0.6909	164	—	3.355	57.25	—
0.1 M inorganic anion	KMnO <sub>4</sub>	0.8318	171.4	16.9	3.624	8.783	7.4
	NaH <sub>2</sub> PO <sub>4</sub>	1.893	21.01	63.5	11.87	26.80	71.7
10 <sup>-2</sup> M amino acid	Valine	5.84	97.0	88.1	29.15	10.91	88.4
	Leucine	1.155	24.52	40.2	49.54	22.87	93.2
	Lysine	8.55	117.5	91.9	108.2	16.46	96.8
50% Green inhibitors	Green water	1.527	131.2	54.7	35.29	40.40	90.4
	Green tea	0.9806	115.5	29.5	17.82	125.0	81.1

TABLE 6

Electrochemical impedance parameters for Cu-Zn alloys in 0.5 M HNO<sub>3</sub> solution in the absence and presence of all investigated inhibitors

Inhibitors		Alloy (I)			Alloy (II)		
		$R_{ct}$ kohm.cm <sup>2</sup>	$C_{dl}$ μF/cm <sup>2</sup>	IE %	$R_{ct}$ kohm.cm <sup>2</sup>	$C_{dl}$ μF/cm <sup>2</sup>	IE %
0.5 M HNO <sub>3</sub> (Blank)		0.1908	466.9	—	0.545	46.13	—
0.1 M inorganic anion	KMnO <sub>4</sub>	0.661	152.1	71.1	1.648	15.25	66.9
	NaH <sub>2</sub> PO <sub>4</sub>	4.628	95.8	96.1	7.954	8.003	93.1
10 <sup>-2</sup> M amino acid	Valine	6.820	32.0	97.2	59.67	29.87	99.0
	Leucine	1.054	16.90	82.9	76.48	7.408	99.2
	Lysine	6.983	91.16	97.4	108.3	8.224	99.4
50% Green inhibitors	Green water	5.105	15.58	96.4	71.44	9.979	99.2
	Green tea	0.2513	63.3	24.1	1.024	1.956	46.7

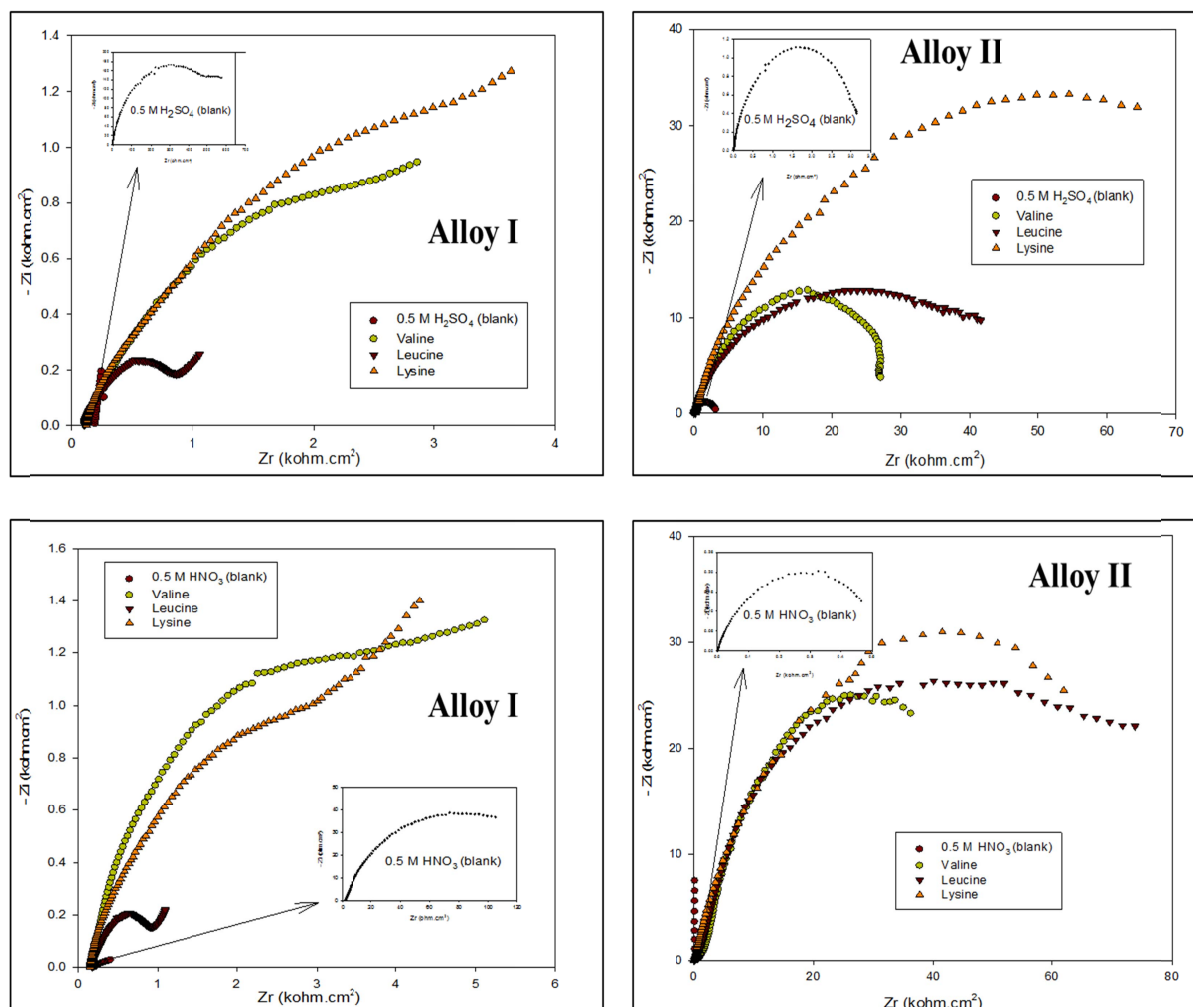


Fig. 8. Nyquist plot for Alloy II in 0.5 M HNO<sub>3</sub> solution in the absence and presence of 0.01 M amino acid

adsorption of inhibitors, and formation of porous layers and in homogenates of the electrode surface [23]. The high frequency limits corresponding to the solution resistance  $R_s$  while the lower frequency limits corresponding to  $R_{ct} + R_s$ . The low frequency contribution showed the kinetic response of the charge transfer reaction [24]. EIS data Tables 5 and 6 show that  $R_{ct}$  values increased for presence of inhibitor than in absence of inhibitor. The adsorption of inhibitors on the electrode surface decreases its electrical capacity as they displace the water molecules and other ions originally adsorbed on the surface. The increase in this capacity with inhibitor may be attributed to the formation of a protective adsorption layer on the electrode surface [21]. Generally, the decrease of the  $C_{dl}$  values Tables 5 and 6, which results from a decrease in local dielectric constant and / or an increase in the thickness of the electrical double layer suggests that the amino acids act by adsorption on the metal/ solution interface.

Figure 9 show Nyquist plots for two Cu-Zn alloys in presence of green water and green tea at 50%. The impedance parameters such as charge transfer resistance  $R_{ct}$ , double layer capacitance  $C_{dl}$  and inhibition efficiency IE% were calculated and are listed in Table 5 and 6. The curves also show a small semicircle in the high frequency region, a large semicircle, which represent the polarization resistance and a tail in the

low frequency region, which represents the present of Warburg impedance components. The charge transfer resistance,  $R_{ct}$ , which is a measure of the resistance of surface towards corrosion of two Cu-Zn alloys, increase with the introduction of the inhibitor. The presence of a small semicircle in high frequency region in the presence of inhibitor suggests the formation of an inhibitor film and Warburg impedance indicates that the system is influenced by mass transfer of corrosion products from the copper surface to bulk [25].

### 3.3. Spectroscopic analysis of Cu-Zn alloys (I and II) in HNO<sub>3</sub> solution

SEM and EDX analyses were used to define the morphology of surface attack and the chemical composition of corrosion products on Cu-Zn alloys from testes terminated just after the film breakdown occurred. The scanning electron microscope images were recorded in Figure 10 to establish the interaction of different components of the extract molecules with the metal surface after exposure in 0.5 M HNO<sub>3</sub> in the absence and presence of 50% of green tea extract. The SEM micrographs of Cu-Zn surface immersed in 0.5 M HNO<sub>3</sub> in Figure 10a and b shows



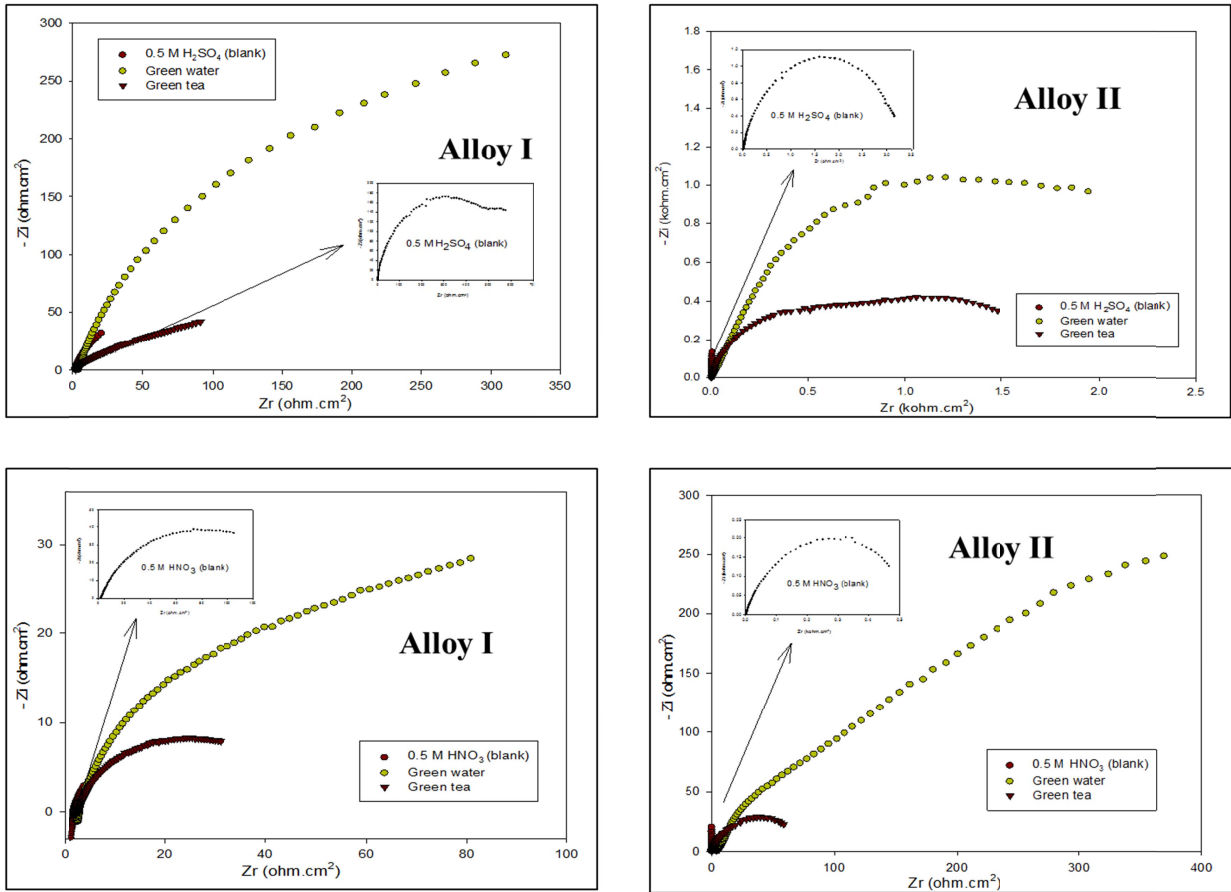


Fig. 9. Nyquist plot for Alloy II in 0.5 M HNO<sub>3</sub> solution in the absence and presence of 50% of green water and green tea

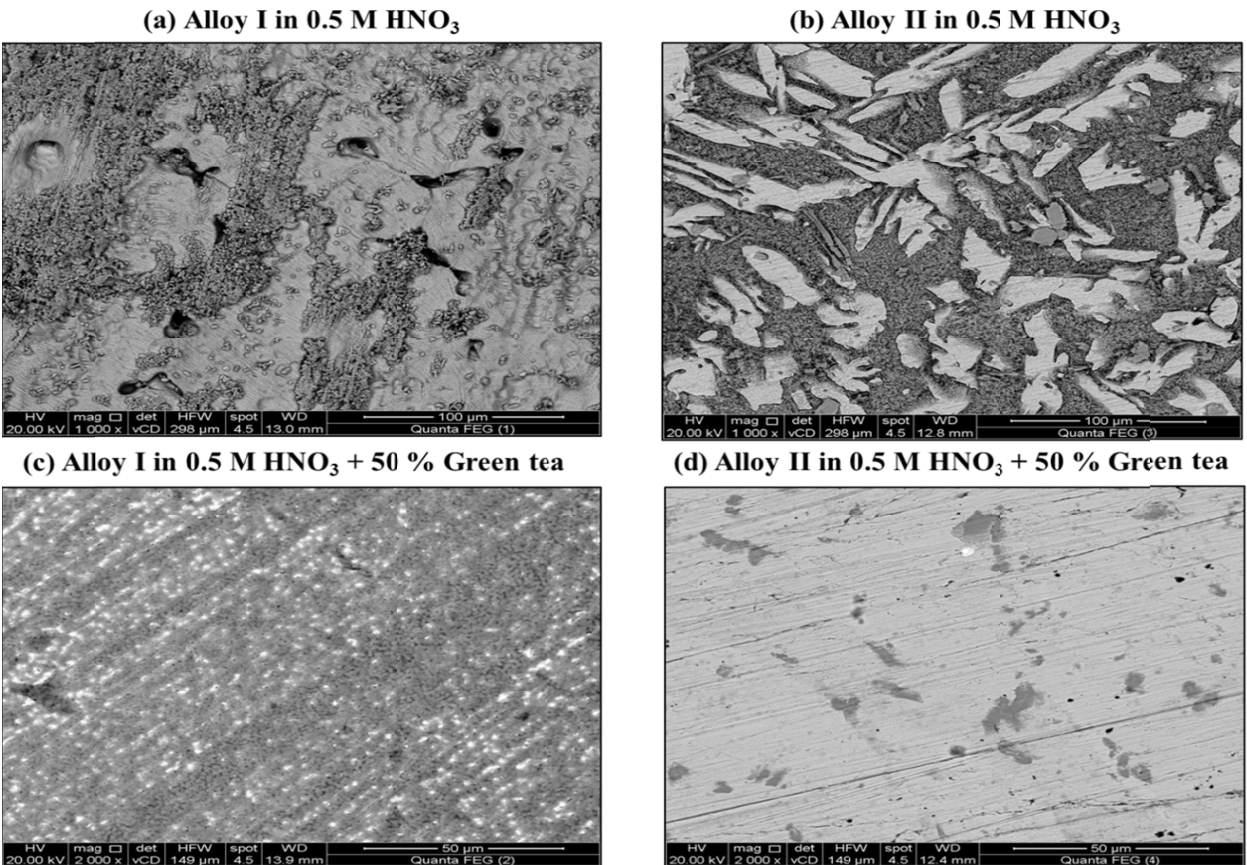


Fig. 10. Surface morphology for the Cu-Zn alloys in 0.5 M HNO<sub>3</sub> solution in the absence and presence of 50% green tea extract

a rough surface covered with corrosion products and appeared like full of pits and cavities. The roughness of the metal surface indicates the corrosion of Cu-Zn alloys in HNO<sub>3</sub>. Figure 10c and d indicates that in the presence of 50% green tea extract the coverage of surface by extract components increases, which in turn results in the formation of insoluble complex on the metal surface and the surface is covered by a thin layer of inhibitor which effectively control the dissolution of Cu-Zn alloys. This indicated that the extract component molecules hinder the dissolution of Cu-Zn alloys by forming an adsorbed layer. The corresponding Energy dispersive X-ray (EDX) profile analysis and percentage of elements presents on the two Cu-Zn alloys in 0.5 M HNO<sub>3</sub> in the absence and presence of 50% green tea extract is presented in Figure 11. The EDX survey spectra were used to determine which elements of inhibitor were present on the electrode surface before and after exposure to the inhibitor solution. For the specimen without inhibitor treatment Figure 11a and b copper, zinc, oxygen for alloy I and II in addition to aluminum especially for alloy II were detected. The main corrosion products formed on exposed copper to nitric acid were identified as the basic copper nitrate, gerhardtite (Cu<sub>2</sub>(NO<sub>3</sub>)(OH)<sub>3</sub>) and to a smaller extent

cuprite (Cu<sub>2</sub>O) [1]. It is noticed the existence of the oxygen peak in the EDX spectra in the case of the two Cu-Zn alloys exposed to the inhibitor, could be attributed to the adsorption of organic moiety at the Cu-Zn surface. The increase in amount of oxygen atom in the case of green tea extract indicated that the dissolution of copper is very inhibited by green tea extract and thereby shows a very high protective capacity. The spectra of Figure 11a and b shows that the oxygen signals are considerably suppressed relative to the Cu-Zn alloys prepared in 0.5 M HNO<sub>3</sub> solution, and certainly this suppression will decrease with addition of investigated inhibitors Figure 11c and d. The increases in oxygen signals takes place due to the overlying inhibitor film. Also it is important to notice the amount of oxygen peaks of EDX spectra is increased in the presence of inhibitor in a comparison of EDX analysis obtained in the absence of inhibitor may indicating that the investigated inhibitor molecules protecting the Cu-Zn surface against acid corrosion, in addition to the surface of the metal may not covered completely by the investigated inhibitors molecules due to the short immersion time. The composition of the detected elements on the Cu-Zn surface indicates that the inhibitor molecules are strongly adsorbed on the copper forming

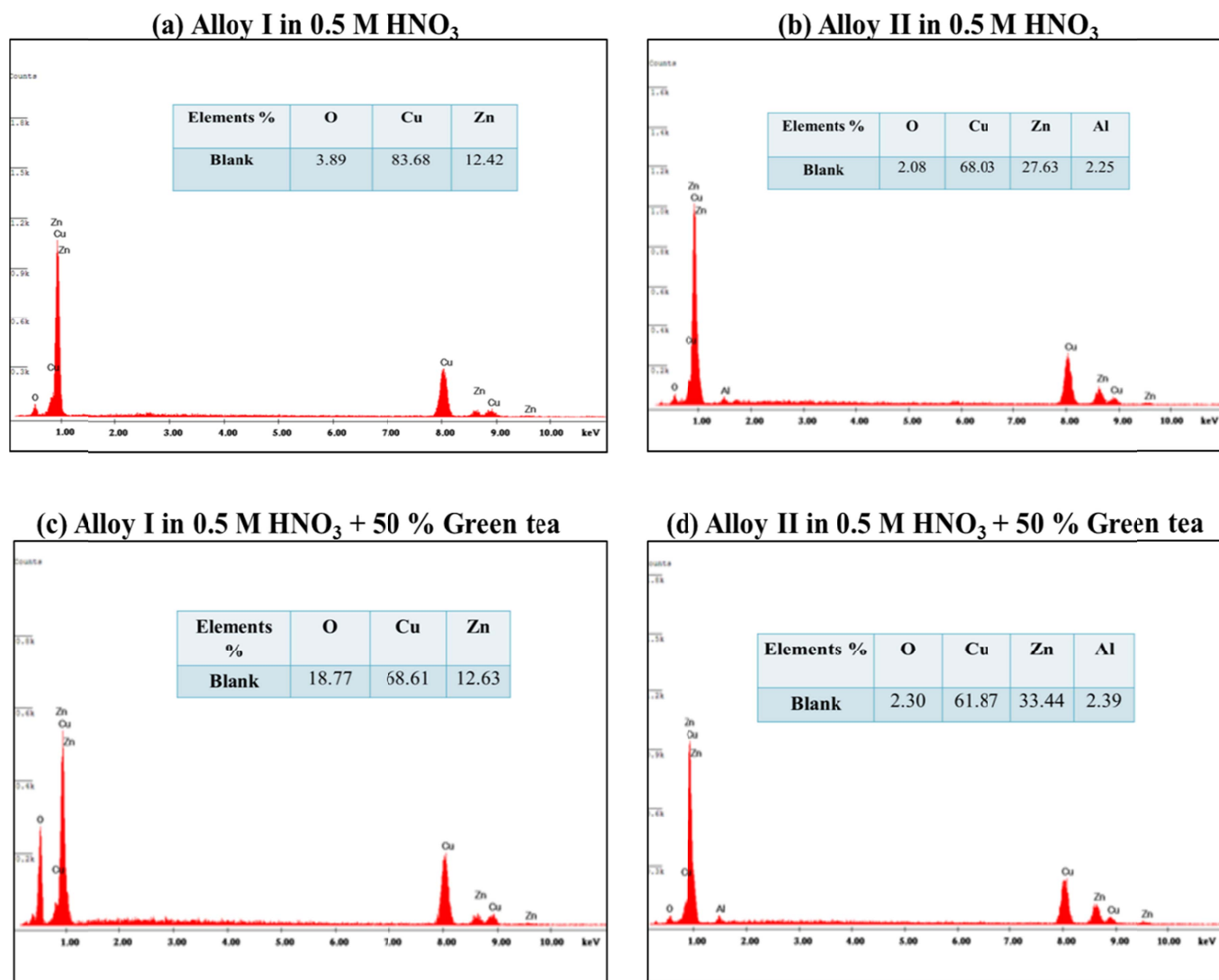


Fig. 11. EDX spectra and percentage of elements present on Cu-Zn alloys in 0.5 M HNO<sub>3</sub> solution in the absence and presence of 50% green tea

a Cu- investigated molecule bond, thus preventing the surface against corrosion.

It is worth to say that, the oxide film formed on Cu-Zn alloys contained copper and zinc in Alloy I and copper, zinc and aluminum in Alloy II. The EDX confirm the formation of protective layer on the Cu-Zn alloys containing aluminum in Alloy II. This sequence reflects the beneficial effects of Al in Alloy II. The presence of 2.43% Al in Alloy II improves the corrosion resistance due to formation of thin, transparent, stable and self – healing  $Al_2O_3$  layer [26]. This confirmed the results obtained from the potentiodynamic polarization measurements and EIS methods.

#### 4. Conclusions

It is important to minimize or control metal corrosion technically, economically and environmentally, which is a major industrial problem. Green corrosion inhibitors are found to be effective from an ecological and environmental perspective and can play a major role over toxic inhibitors. In this article we evaluate some inorganic anion and organic compound as corrosion inhibitors for protection two Cu-Zn alloys in oxy acid solution. It found that, potassium permanganate and di-hydrogen phosphate improve corrosion resistance of the two Cu-Zn alloys. Phosphate appears more effective as corrosion inhibitor for the Cu-Zn alloys I and II than permanganate. It is still amazing that the anticorrosion efficiency of green corrosion inhibitors are equal to or even more effective than synthetic inhibitors. The addition of small amounts of naturally occurring amino acids compound at  $10^{-2}$  reduce the corrosion rate of two Cu-Zn alloys in  $H_2SO_4$  or  $HNO_3$  solution. The amino acid acts as effective inhibitor, especially for lysine and corrosion inhibition efficiency,  $IE\%$ , of  $\sim 87$  and  $\sim 59$  is for  $H_2SO_4$  and  $\sim 96.3$  and  $54.9$  for  $HNO_3$  for alloy I and II respectively are observed. The inhibition efficiency,  $IE\%$ , on the two Cu-Zn alloys in presence of cooling green water reaching 91.8 and 96.5% for Alloy I and 95.4 and 87.1% for Alloy II in 0.5 M  $H_2SO_4$  and  $HNO_3$  respectively. Although benzotriazole, in cooling green water, is excellent inhibitor suitable for use in wide variety of environments, it has toxic properties. So, much of recent researches have focused on formulating new and more environmentally acceptable preservation solutions. The green tea, as plant extract, will be very environmentally friendly. Natural products as green corrosion inhibitors having the limitation of their production volume on larges industrial scales, therefore, their economic aspects must be evaluated for industrial usage. The EDX confirm the formation of protective layer on the Cu-Zn alloys containing aluminum in Alloy II. This sequence reflects the beneficial effects of Al in Alloy II. The presence of 2.43% Al in Alloy II improves the corrosion resistance due to formation of thin, transparent, stable and self – healing  $Al_2O_3$  layer. This confirmed the results obtained from the potentiodynamic polarization measurements and EIS methods.

#### Acknowledgements

The authors acknowledge the support extended by Central Metallurgical Research and Development Institute (CMRDI), Al – Tabbin, Helwan.

#### REFERENCES

- [1] W.A. Hussein, A.S.I. Ahmed, W.A. Ghanem, Gh.A. Gaber, Journal of Metallurgical Engineering (ME) **5**, 27-37 (2016).
- [2] K. Ghulamullah, K.M.S. Newaz, W.J. Basirun, A.B. M. Hapi-pah, F.L. Faraj, K.Gh. Mustafa, Inter. J. Electrochem. Sci. **10**, 6120-6134 (2015).
- [3] V.S. Sastri, Corrosion Inhibitors, Principle and Application, John Wiley and sons, New York, 33 (1998).
- [4] S.A. Ali, H.A. Al-Muallem, S.U. Rahman, M.T. Saeed, Corros. Sci. **50**, 3070-377 (2008).
- [5] P.B. Raja, M.G. Sethuraman, Mater. Lett. **62**, 113-116 (2008).
- [6] A.M. Abdel-Gaber, E. Khamis, H. Abo-ELDahab, Sh. Adeel, Mater. Chem. Phys. **109**, 297-305 (2008).
- [7] A.R. Afidah, E. Rocca, J. Steinmetz, M.J. Kassim, Corros. Sci. **50**, 1546-1550 (2008).
- [8] Gh. A. Gaber, M. A. Maamoun, W. A. Ghanem, Key Engineering Materials **786**, 174-194 (2018).
- [9] W.A. Ghanem, I.M. Ghayad, Gh.A. Gaber, International Journal of Metallurgical & Materials Science and Engineering (IJMMSE) **3** (5), 1-8 (2013).
- [10] Y.M. Abdallah, H. M. Hassan, K. Shalabi, A.S. Fouda, Inter. J. Electrochem. Sci. **9**, 5073-5091 (2014).
- [11] K.M. Ismail, Electrochimica Acta **52**, 7811-7819 (2007).
- [12] R. Rosliza, W.B. Wan Nik c, S. Izman d, Y. Prawoto, Current Applied Physics **10**, 923-929 (2010).
- [13] V. Subramanian, P. Chandramohan, M.P. Srinivasan, S. Velmurugan, S.V. Narasimhan, Corros. Sci. **49**, 620-636 (2007).
- [14] N.K. Allam, E.A. Ashour, Mater. Sci. Eng. B **156**, 84-89 (2009).
- [15] E.A. Ashour, B.G. Ateya, Corros. Sci. **37** (3), 371-380 (1995).
- [16] K. Barouni, L. Bazzi, R. Salghi, M. Mihit, B. Hammouti, A. Al-bourine, S. El Issami, Mater. Lette. **62**, 3325-3327 (2008).
- [17] A.A. Aksut, S. Bilgic, Corros. Sci. **33** (3), 379-387 (1992).
- [18] W.A. Badawy, K.M. Ismail, A.M. Fathi, Electrochimica Acta **51**, 4182-4189 (2006).
- [19] N.K. Allam, A. Abdel Nazeer, E. A. Ashour, J Appl. Electrochem. **39** (7), 961-969 (2009).
- [20] N. Souissi, E. Triki, J. Mater. Sci. **42**, 3259-3265 (2007).
- [21] D. Özkler, E. Bayol, A. A. Gürten, Y. Surme, F. Kandemirli, Chem. Pape. **67** (2), 202-212 (2013).
- [22] A.M. Shah, A.A. Rahim, S.A. Hamid, S. Yahya, Inter. J. Electrochem. Sci. **8**, 2140-2153 (2013).
- [23] A.S. Fouda, K. Shalabi, H. Elmogazy, J. Mater. Environ. Sci. **5** (6), 1691-1702 (2014).
- [24] F. Mansfeld, Electrochim. Acta. **35**, 1533 (1990).
- [25] R. Senthoooran, N. Priyantha, Ann. Res. J. SLSAJ **12**, 01-10 (2012).
- [26] M. Pourbaix, Atlas of Electrochemical Equilibria, Pergamon, Oxford, (1966).